Journal of Molecular Liquids 413 (2024) 125986

Contents lists available at ScienceDirect

Journal of Molecular Liquids

journal homepage: www.elsevier.com/locate/molliq

High efficacy of chloroquine-derived bile salts in Pluronic F127 micelles against blood-stage *Plasmodium falciparum*

Ana Teresa Silva [a], Isabel S. Oliveira [b], Inês Morais [c], Sofia Santana [d], Eyob A. Workneh [d], Miguel Prudêncio [d], Fátima Nogueira [c], Ricardo Ferraz [a,e,f], Paula Gomes [a], Eduardo F. Marques [b,*]

[a] *LAQV-REQUIMTE, Departamento de Química e Bioquímica, Faculdade de Ciências, Universidade do Porto, P-4169-007 Porto, Portugal*
[b] *CIQUP, IMS (Institute of Molecular Sciences), Departamento de Química e Bioquímica, Faculdade de Ciências, Universidade do Porto, P-4169-007 Porto, Portugal*
[c] *Universidade NOVA de Lisboa, UNL, Global Health and Tropical Medicine, GHTM, Associate Laboratory in Translation and Innovation Towards Global Health, LA-REAL, Instituto de Higiene e Medicina Tropical, IHMT, Rua da Junqueira 100, 1349-008 Lisboa, Portugal*
[d] *Instituto de Medicina Molecular, Faculdade de Medicina Universidade de Lisboa, P-1649 028 Lisboa, Portugal*
[e] *Ciências Químicas e das Biomoléculas, Escola Superior de Saúde - Instituto Politécnico do Porto, P-4200-072 Porto, Portugal*
[f] *Centro de Investigação em Saúde Translacional e Biotecnologia Médica (TBIO)/Rede de Investigação em Saúde (RISE-Health), Escola Superior de Saúde, Instituto Politécnico do Porto, R. Dr. António Bernardino de Almeida, 400, 4200-072 Porto, Portugal*

ARTICLE INFO

Keywords:
Antimalarial drugs
Surface-active ionic liquids
Chloroquine & bile salts
Polymeric and mixed micelles
Drug nanocarriers
Antiplasmodial activity

ABSTRACT

Colloidal nanocarriers can play a key role in the efficacious delivery of drugs, including antimalarials. Here, we investigated the ability of polymeric micelles of the block copolymer F127 to act as nanovehicles for two organic salts derived from chloroquine and human bile acids, namely, chloroquinium cholate (iCQP1) and chloroquinium glycocholate (iCQP1g). We have previously reported the strong *in vitro* antiplasmodial activity of these salts, which displayed IC_{50} values of 13 and 15 nM against blood forms of *Plasmodium falciparum*, respectively. By deriving from amphiphilic lipids, iCQP1 and iCQP1g also enclose the ability to act as surface-active ionic liquids (SAILs). The micellization properties of neat F127 and of the F127/SAIL mixtures were initially investigated to gain physicochemical insight into the interaction between polymer and bioactive SAILs, resorting to differential scanning calorimetry, surface tension measurements and dynamic light scattering. Micelle formation by F127 is an endothermic process strongly temperature and concentration dependent. Interestingly, this process is significantly changed when the molar fraction of SAIL (x_{SAIL}) in the F127/SAIL mixture is varied between 0.33 and 0.90. Both SAILs favor the formation of mixed micelles by decreasing the micellization temperature, and (observed only when for $x_{SAIL} = 0.33$) by synergistically decreasing the *cmc*. Concomitantly, the micellar size is reduced from 18 to 13 nm as x_{SAIL} is increased from 0.33 to 0.90. Crucially, *in vitro* assays show that when the SAILs are loaded into F127 polymeric micelles, their antiplasmodial efficacy is substantially enhanced, with a significant drop in IC_{50}, especially for the iCQP1/F127 system. This opens new possibilities for the nano-formulations of antimalarial compounds.

1. Introduction

Malaria, a parasitic infection caused by *Plasmodium* spp. parasites, has significantly impacted human populations for centuries. Despite the latest vigorous prevention and treatment efforts, this disease continues to affect countless lives, particularly in Africa, which accounts for about 94 % of global malaria cases. In 2022 only, *Plasmodium* infections resulted in approximately 249 million cases of malaria and an estimated 608,000 deaths [1], with major socio-economic impacts in affected countries. One contributing factor for such danger is the emergence of drug resistance resulting from, among other factors, exposure of the parasite to low drug doses [2–4]. Hence, there is an ongoing need for novel therapeutic options that are cost-effective and preferentially target multiple stages of the parasite's life cycle to improve therapeutic efficiency and minimize the risk of resistance.

Drug recycling is an approach that explores existing approved or rejected drugs in an effort to make drug development less costly and time-consuming than *de novo* drug development [5–7]. In this context,

* Corresponding author.
E-mail address: efmarque@fc.up.pt (E.F. Marques).

https://doi.org/10.1016/j.molliq.2024.125986
Received 22 July 2024; Received in revised form 30 August 2024; Accepted 10 September 2024
Available online 12 September 2024

we have recently reported the combination of basic antimalarials like chloroquine and primaquine with different natural lipids, including fatty acids [8,9] and bile acids [10], to produce organic salts (ionic liquids, ILs) with renewed antiplasmodial activity. We have previously hypothesized that these drug-derived organic salts, by virtue of incorporating amphipathic lipids, would behave as surface-active ionic liquids (SAILs) with enhanced delivery *in vivo* as compared to the parent antimalarials [8–10]. Most reports on ILs that are able to enhance drug delivery refer to topical or transdermal administration, whereas the efficacy of ILs administered via other routes remain much less explored [11]. Still, there is growing evidence that oral delivery of drugs may be substantially enhanced by use of ILs [12], including SAILs possibly in combination with other surfactants [13]. As such, we have now explored the self-assembling properties of two antimalarial chloroquine-derived bile salts (Fig. 1), namely, chloroquinium cholate (iCQP1) and chloroquinium glycocholate (iCQP1g) [10], alone and in combination with a nanocarrier system [14,15].

Colloidal nanocarriers can play a pivotal role in the efficacious delivery of drugs, including antimalarials. Such nanocarriers protect the drug from degradation and enhance targeted drug delivery, reducing the exposure of healthy cells and mitigating toxicity effects, while ensuring sufficient local doses enough to quickly eliminate parasites and avoid the development of resistance [16]. Various antimalarial drugs have been encapsulated in different types of colloidal nanocarriers, including liposomes [17,18], polymeric micelles [19] and dendrimers [20,21], providing positive results that encourage further use of nanotechnological approaches in malaria [22,23]. Among the wide diversity of drug nanocarriers, polymeric micelles have been gaining traction given their capacity to solubilize hydrophobic drugs and to enhance their bioavailability, while offering stability through a robust core–shell structure [24,25]. These micelles (like all micellar types, irrespective of composition) are thermodynamically stable aggregates, but unlike surfactant micelles, they present slow dynamics (e.g. high micelle lifetime and high unimer residence time), which is useful in the context of drug delivery, namely, to improve oral bioavailability [26]. Overall, slow dynamics results in the preserved integrity of the micelles before getting to the target sites [27]. Pluronic polymers, also known as poloxamers, constitute a family of amphiphilic triblock copolymers frequently used to form polymeric micelles in aqueous media. They are composed of poly(propylene oxide) (PPO) and poly(ethylene oxide) (PEO) as hydrophobic and hydrophilic monomeric units, respectively, and have a common (PEO)x-(PPO)y-(PEO)x architecture. Due to their amphiphilic character, in aqueous solutions, at a fixed temperature and at concentrations above the critical micellization concentration (cmc), Pluronic molecules form micelles with the hydrophilic PEO segments facing the water and the PPO segment facing inwards into the micellar core [28]. Given their high levels of biocompatibility and biodegradability, interfacial and self-assembling properties, some of these polymers are approved by the U.S. Food and Drug Administration (FDA) for use in pharmaceutical formulations. One such polymer that is widely used is Pluronic F-127 (F127) (Fig. 1) [29]. F127 has been exploited to improve the oral bioavailability of several drugs [26,30–33], including in nanoformulations of the emblematic antimalarial drug artemisinin [34].

In view of all the above, herein, we investigated the interaction of the chloroquine bile salts iCQP1 and iCQP1g with F127 micelles in aqueous solution, aimed at the unveiling of an efficient and robust nanocarrier system. These micelle-based formulations were screened *in vitro* against the blood stage of *P. falciparum* parasites, showing a clear enhancement of antiplasmodial action as compared to the parent compounds.

2. Experimental section

2.1. Materials and sample preparation

The synthesis of the iCQP1 and iCQP1g SAILs was performed according to the neutralization method previously reported by us [10]. Pluronic® F-127 (Poloxamer 407) was purchased from Sigma-Aldrich and used without further purification. The solutions of polymer, SAILs, and polymer/SAIL mixtures were prepared by directly weighing both the solutes and solvent (water) in vials, followed by appropriate stirring at the desired temperature until complete dissolution of the compounds. Due to this procedure, the concentration of solute is expressed in molality (number of moles of solute per mass of solvent in kg). The stock solutions of polymer were prepared with a fixed concentration of 5.0 mmol·kg^{-1} by dissolution of F127 in ultrapure Milli-Q® water at room temperature. The F127/SAIL mixtures were prepared by dissolving solid SAIL in F127 micellar solution, followed by vigorous stirring for 24 h. The molar fraction of SAIL expresses the relative proportion of the two solutes in the system according to the definition:

$$x_{\mathrm{SAIL}} = n_{\mathrm{SAIL}}/(n_{\mathrm{SAIL}} + n_{\mathrm{F127}}) \quad (1)$$

where n_{SAIL} and n_{F127} are the number of moles of the SAIL and F127, respectively.

For the biological assays, for convenience and comparison with previous studies, the stock solutions were prepared using volumetric flasks, and appropriately diluted by volume, and concentrations are thus expressed in molarity (number of moles of solute per volume of solution in dm^3).

2.2. Differential scanning microcalorimetry (DSC)

DSC experiments were conducted using a properly calibrated MicroCal VP-DSC microcalorimeter, at a scanning rate of 1.5 °C·min^{-1}. Before sample loading, blank runs (ultrapure Milli-Q® water in both cells) were done for baseline correction. Various heating–cooling cycles were carried out, to determine the phase transition parameters of F127 and F127/SAIL mixtures, and to investigate the reversibility of the aggregation process. Analysis of the DSC thermograms allowed to retrieve the critical micellization temperature (*cmt*) as well as to determine the molar enthalpy ($\Delta_{\mathrm{mic}}H_{\mathrm{m}}$) and entropy ($\Delta_{\mathrm{mic}}S_{\mathrm{m}}$), of micellization. For the observed micellization peak, both the onset temperature (T_{on}) and the temperature at peak maximum (T_{max}) were determined.

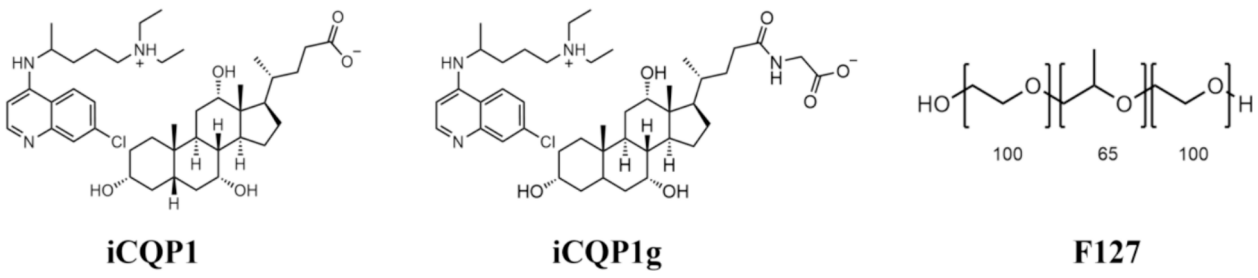

Fig. 1. Molecular structures of chloroquinium cholate (iCQP1), chloroquinium glycocholate (iCQP1g), and triblock copolymer Pluronic F-127 (F127), with a poly (ethylene oxide)/poly(propylene oxide)/poly(ethylene oxide) (PEO-PPO-PEO) structure.

2.3. Surface tension

A DCAT11 tensiometer from Dataphysics GmbH with a Pt–Y alloy Wilhelmy plate and a thermostated Julabo F20 circulating bath was used for determining the *cmc* of F127 and of the F127/SAIL mixtures. The assays involved adding aliquots from a stock solution to the solution in the measuring vessel (starting with only ultrapure Milli-Q® water) and then conducting the measurements. For the neat surfactants, the *cmc*, the surface tension at that point (γ_{cmc}), and the minimum surface area per molecule ($a_{s,min}$), calculated from Eqs. (2) and (3), were determined. For the F127/SAIL mixtures, it was only possible to determine *cmc* and γ_{cmc}. The Gibbs isotherm equation applied to a surfactant solution may be expressed as:

$$\Gamma_s = -\frac{1}{nRT}\left[\frac{\partial\gamma}{\partial \ln(c_s/c^\circ)}\right]_{p,T} \quad (2)$$

where Γ_s is the surface excess concentration of surfactant (for zero surface excess of the solvent), R is the gas constant, T is the absolute temperature, n is the number of adsorbed species obtained from the surfactant at the interface (Gibbs pre-factor) and $\partial\gamma/\partial\ln(c_s/c^\circ)$ is the local slope of the γ *vs.* $\ln(c_s/c^\circ)$ curve, where c_s is the surfactant molal concentration and $c^\circ = 1$ mol·kg^{-1}. The minimum surface area per surfactant molecule, $a_{s,min}$, is calculated from:

$$a_{s,min} = \frac{1}{\Gamma_{s,max}\, N_A} \quad (3)$$

where N_A is Avogadro's constant and $\Gamma_{s,max}$ is the maximum surface excess calculated for the biggest slope of the γ *vs.* $\ln(c_s/c^0)$ curve prior to the *cmc* inflection point.

2.4. Dynamic light scattering (DLS)

The size (mean diameter, $\langle D_h \rangle$) and zeta potential (ζ-potential) were measured using a Litesizer 500 from Anton Paar, equipped with the Kalliope software. A laser diode (658 nm) was used as the light source, with automatic adjustment of the scattering angle. The experiments were performed in disposable polystyrene cuvettes for size determinations and Ω-shaped ζ-potential cuvettes at 25 °C. Either the cumulant and CONTIN algorithm methods were used to analyze the intensity auto-correlation function plots obtained, depending on sample polydispersity [35,36]. The electrophoretic mobility, μ, was measured using a combination of electrophoresis and laser Doppler velocimetry techniques, and the zeta potential was calculated from μ by applying Smoluchowski's model, with a Henry's function value $f(\kappa\alpha) = 1.5$, under Smoluchowski's approximation [36].

2.5. In vitro antimalarial activity

A laboratory-adapted *P. falciparum* 3D7-GFP (MRA-1029, MR4, ATCC® Manassas, VA, USA), a chloroquine-sensitive strain expressing the green fluorescent protein, was continuously cultured, as reported previously [37]. Parasitemia was assessed by light microscopy of Giemsa-stained thin blood smears. Antiplasmodial activity assessment was performed using a modification of SYBR Green I assay [38]. Briefly, unsynchronized cultures with 0.6 % hematocrit and 0.5 % parasitemia were incubated with the test compounds (iCQP1 and iCQP1g) in 3-fold serial dilutions ranging from 729 to 1 nM at constant F127 concentration (10, 20 and 30 μM), in a 96-well flat bottom plate, for 72 h (37 °C and 5 % CO_2). Parasite growth was assessed by flow cytometry (Beckman Coulter, Cytoflex) with a 96-well plate reader using Fl-1 (GFP) [39]. Typically, 100,000 erythrocytes were counted for each well and the samples were analyzed with the FlowJo software (Tree Star Inc.). Half-maximal inhibitory concentrations (IC_{50}) were determined with GraphPad Prism 5 (trial version). At least three experiments, each in duplicate, were performed to obtain the mean IC_{50} values presented.

2.6. Hemolytic activity

Human blood samples were centrifuged (Centurion scientific Ltd centrifuge with a BRK1011) for 5 min at 1020 g and at 4 °C to remove the plasma. Erythrocytes were then washed (×3) with phosphate buffer saline solution (PBS, 0.01 M, pH 7.4), and diluted to a final volume fraction of 4 % hematocrit in PBS. Then, the red blood cells (100 μL, 4 %) were plated in a 96-well plate in the presence of 100 μL of the test compound (at different concentrations) in PBS with ultrapure (Milli-Q®) water 80/20 v/v. The following controls were used: positive control, 1 % Triton X-100 in PBS; negative controls, PBS and PBS with ultrapure (Milli-Q®) water 80/20 v/v. The plate was incubated at 37 °C for 1 h, after which the absorbance of the supernatant at 540 nm was measured in a multi-mode microplate reader (Multiskan GO-Thermo Scientific). The hemolytic activity was calculated using the following equation, where A stands for UV/Vis absorbance:

$$Hemolysis\ \% = \frac{A(\text{sample}) - A(\text{PBS 80/20 v/v})}{A(\text{positive control}) - A(\text{PBS})} \times 100 \quad (4)$$

Ethics statement: The human blood was provided from Serviço de Hematologia Clínica do Centro Hospitalar Universitário do Porto through a collaboration protocol with our group. The blood was submitted the necessary analytical checks as required by current legislation before the assay. The data associated with each unit were anonymized and irreversibly dissociated before delivery. The only information provided were the donor's date of birth, blood group, and sex. The blood was used exclusively in the assays explicit in this research.

3. Results and discussion

3.1. Characterization of F127 micellization

It was relevant to establish the main characteristics of the neat polymeric F127 micelles before evaluating their use as nanocarriers of the antimalarial SAILs iCQP1 and iCQP1g. Though the micellization of F127 has been reported previously [40–45], the exact nature of the polymer composition, the solution conditions, and the techniques used vary widely from one report to another. Given that the micellization process of F127 is a first order phase transition, it was conveniently quantitatively investigated by DSC, and the results thus obtained are shown in Fig. 2a-d.

Upon heating, the transition between the unimer and micellar states of the polymer solution shows as a broad endothermic peak, as observed in Fig. 2a. Moreover, the temperature of formation of F127 micelles depends markedly on polymer concentration, as is common for nonionic amphiphiles. A phase diagram can be drawn as shown in Fig. 2b, where the temperature/concentration coupling can be more easily seen and both the *cmt* and the *cmc* can be read. At a given polymer concentration, micelles form above a certain temperature, the *cmt*, and at a given temperature, the polymer form micelles only above a certain concentration, the *cmc*. As the concentration of polymer increases, the micellization process becomes increasingly favorable and the *cmt* decreases. The micellization process is characterized by an average $\Delta_{mic}H_m = 301 \pm 8$ kJ·mol^{-1} and an average $\Delta_{mic}S_m = 1015 \pm 24$ J·K^{-1}·mol^{-1}.

F127 was also studied regarding its surface activity through surface tension measurements at varying polymer concentration and at constant temperature. This temperature was set to 26.5 ± 0.1 °C, slightly above room temperature for technical convenience, and the value obtained for the *cmc* is 0.18 ± 0.01 mmol·kg^{-1}, as shown in Fig. 2c. When the DSC upscan was run (at a heating rate of 1.5 °C·min^{-1}) for an aqueous solution of F127 at 0.18 mmol·kg^{-1}, the broad endothermic peak is characterized by an onset temperature, T_{on}, of 26.5 °C and a peak temperature, T_{max}, of 30.9 °C (Fig. 2d). Thus, T_{on} was henceforth taken as the characteristic micellization temperature, and the DSC and surface tension measurements were confirmed as mutually consistent. Table S1 in the supporting information (SI) shows the detailed thermodynamic

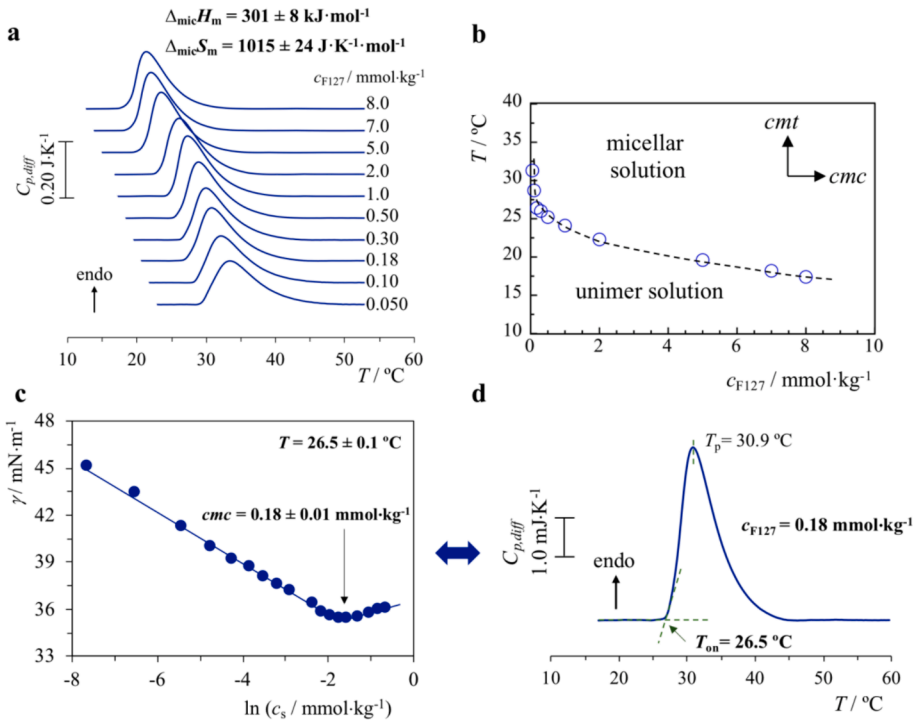

Fig. 2. Micellization process of polymer F127: **a**, DSC thermograms obtained as a function of polymer concentration, at a scanning rate of 1.5 °C·min^{-1}, with indication of the average molar enthalpy and average molar entropy of micellization obtained; **b**, temperature *vs.* concentration phase diagram of F127, where both the critical micelle temperature (*cmt*) and the critical micelle concentration (*cmc*) can be read; **c**, surface tension curve of F127 at 26.5 °C, yielding a *cmc* of 0.18 mmol·kg^{-1}; **d**, DSC thermogram of a F127 solution at 0.18 mmol·kg^{-1}, yielding T_{on} = 26.5 °C and T_{max} = 30.9 °C. T_{on} is thus considered as the critical micellization temperature, *cmt*.

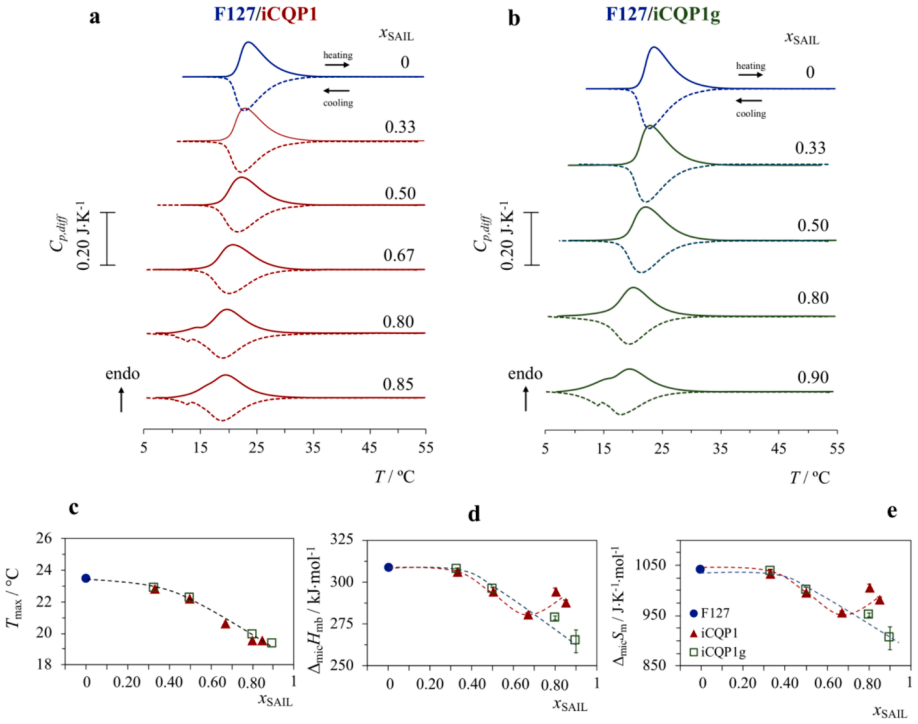

Fig. 3. Effect of increasing molar fraction of SAIL, x_{SAIL}, on the micellization behavior of F127/SAIL mixtures as probed by DSC: **a**, thermograms of F127/iCQP1 system, with both heating and cooling scans shown; **b**, DSC thermograms of F127/iCQP1g system, with both heating and cooling scans shown; **c**, **d**, and **e**, calculated thermodynamic parameters—respectively, temperature, molar enthalpy and molar entropy of micellization—obtained *vs.* x_{SAIL}.

data obtained for the DSC studies between 0.050 and 8.0 mmol·kg^{-1} (0.063–9.1 wt%).

3.2. Formation of mixed micelles of F127 and chloroquine bile salts

3.2.1. DSC studies

In order to evaluate the capacity of the F127 micelles to act as nanocarriers of the chloroquine bile salt SAILs, the next step was to investigate the F127/SAIL interactions in solution, resorting to DSC, DLS, and surface tension measurements. It should be noted first that both iCQP1 and iCQP1g are not only surface-active molecules, but they also self-assemble into micellar aggregates, showing *cmc* values of 0.60 and 0.78 mmol·kg^{-1}, respectively, as determined by surface tension measurements (results shown further ahead in this section). Therefore, we investigated whether each SAIL can co-aggregate with the F127 micelles.

One of the most straightforward ways to assess interactions as those herein under study is to perform DSC analysis of mixtures of F127, at a constant concentration, with SAIL at increasing molar fraction and monitor the effect (if any) of the SAIL on the original DSC profile of F127 alone. The mixtures of F127 and SAILs were prepared at fixed value of c_{F127} = 5.0 mmol·kg^{-1} (T_{on} = *cmt* = 19.6 °C), while varying x_{SAIL} between 0.33 and 0.90. These conditions were selected to ensure that, at or above room temperature ($T \geq 25$ °C), (i) the polymer is in micellar form (since $T >$ *cmt*) and (ii) the DSC signal is strong enough to gauge the effect of even small fractions of added SAIL. It should be also noted that none of the SAILs (also micelle-forming surfactants) showed any transition peak in the temperature range investigated (5 – 60 °C).

Fig. 3a and b show the thermograms of the F127/iCQP1 and F127/iCQP1g mixtures, respectively, for varying molar fraction of SAIL. The values obtained for T_{max}, $\Delta_{mic}H_m$ and $\Delta_{mic}S_m$ are shown in Fig. 3c, d and e, respectively. In both systems, it is clear that as increasing amounts of SAIL are present, the micellization becomes increasingly affected and this can only be caused by a strong association between the polymer and the SAIL, i.e. the formation of mixed F127/SAIL micelles.

Several aspects, (i)–(v), of the DSC results can be highlighted. (i) As the quantity of SAIL increases, the endothermic micellization peak becomes broader, which suggests a more gradual micellization process. For this reason, in Fig. 3c, T_{max} (instead of T_{on}) is plotted *vs.* x_{SAIL}. (ii) The reversibility of the aggregation in all mixtures is demonstrated by the fact that the heating and cooling peaks are nearly mirror images of each other, with only a very small undercooling of the exothermic (cooling) peak. (iii) As x_{SAIL} increases, the endothermic peak shifts to lower temperature, indicating that micellization is thermally favored when SAIL molecules are incorporated in the micelles. For both mixtures, the T_{max} decreases from 23.5 °C (original value for F127) down to about 19 °C when an x_{SAIL} = 0.80 is reached. Interestingly, at very high x_{SAIL}, for iCQP1 at 0.80 and 0.85 and for iCQP1g at 0.90, a satellite peak, at about 14–15 °C, appears. This suggests that more than one type of micelle is present, likely F127-rich micelles, for the main peak, and SAIL-rich ones, for the weaker peak. (iv) A similar decreasing trend is observed both in the molar enthalpy and the molar entropy of micellization (calculated per mole of F127) as x_{SAIL} increases. For F127/iCQP1, the behavior is slightly distinct at 0.80 and 0.85, with $\Delta_{mic}H_m$ and $\Delta_{mic}S_m$ undergoing a slight uptrend. This effect is qualitatively consistent with the temperature trend described above, likely assignable to the SAIL-saturated F127-rich micelles and formation of SAIL-rich micelles. (v) In any phase transition $\Delta_{tr}G$ = 0 and thus $T_{tr} = \Delta_{tr}H/\Delta_{tr}S$. In the current systems, the fact that T_{max} decreases with growing amounts of incorporated SAIL implies that the decrease in $\Delta_{mic}S_m$ is stronger than the decrease in $\Delta_{mic}H_m$. How to fathom this trend at molecular level? The formation of F127 micelles is driven by the hydrophobic effect, an entropic effect associated with water structure as the nonpolar segments of the polymer are removed from the contact with bulk water into the micellar core. Clearly, the SAIL molecules, being much smaller than the polymer molecules, will make the entropic gain per mole of F127 associated with the polymer micellization less than optimal. This effect will be more significant as the SAIL molecules become more abundant in the system.

3.2.2. Surface tension studies

To gain further insight into the F127/SAIL interactions and corroborate the mixed micellization suggested by DSC analysis, surface tension studies were conducted on the mixtures, affording the results that are shown in Fig. 4 and Table 1.

First, we analyze the results of the neat F127 and SAILs, as well as of the bile salts sodium cholate (NaP1) and sodium glycocholate (NaP1g), for comparisons; data for these single-solute systems are all shown in Fig. 4a, for T = 26.5 °C. The polymer has the smallest *cmc* of the set, 0.18 mmol·kg^{-1}, by virtue of its extensive hydrophobic group, the PPO middle block. The SAILs also have comparatively small *cmc* values, 0.60 and 0.78 mmol·kg^{-1} for iCQP1 and iCQP1g, respectively, and much smaller (more than one order of magnitude) than their comparable sodium bile salts, NaP1 and NaP1g. Therefore, replacing the sodium cation in bile salts with the chloroquinium cation in the SAILs results in a significant decrease of *cmc*. This is not surprising: the chloroquinium cation is a big organic amphiphilic ion and thus it co-aggregates with cholate or glycocholate into virtually uncharged catanionic micelles, unlike the small inorganic Na^+ counterions that are partially dissociated from the bile salt micelles, making them net anionic micelles. In other words, while the sodium bile salts behave as anionic surfactants in solution, their corresponding chloroquine-derived SAILs behave as essentially neutral ones, and thus are expected to have significantly lower *cmc* than the former, as the absence of electrostatic repulsions between charged headgroups makes micellization thermodynamically much more favorable.

It is also interesting to observe from the data in Table 1 that the SAILs are much more surface-active than the corresponding sodium bile salts, as evident from the much lower values of both the minimum interfacial molecular area, $a_{s,min}$, and the surface tension at the *cmc*, γ_{cmc}. This is also true with respect to F127, even though in this case the comparison is less meaningful, because this polymer and SAILs have very different chemical structure and size. Furthermore, the same relative order of *cmc* is seen between similar compounds, that is, *cmc* (iCQP1) < *cmc* (iCQP1g) and *cmc* (NaP1) < *cmc* (NaP1g). This trend is also logical, as glycocholate headgroup is more hydrophilic than cholate, on account of the amide group in the former, capable of H-bonding with water. This will tend to make glycocholate-derived unimers more water-soluble which, together with the higher steric hindrance between headgroups at the micellar surface, delays micellization.

For the F127/SAIL mixtures, shown in Fig. 4b and c, two compositions were analyzed, one richer in F127, x_{SAIL} = 0.33, and another richer in SAIL, x_{SAIL} = 0.80. The results are rather significant. First, the surface tension curves of the mixtures, where c_s now represents the total concentration of F127 + SAIL, confirm the strong interactions between F127 with each SAIL, already detected by DSC. For x_{SAIL} = 0.33, two break points in the *cmc* curve can be seen (signaled by the two arrows), one at fairly low c_s (0.022 and 0.011 mmol·kg^{-1} for iCQP1 and iCQP1g, respectively) and the other close to the *cmc* value of neat F127. The existence of two inflection points in surface tension curves of surfactant mixtures has been reported before [46–50], and they are associated to distinct events of aggregation. Here, the first one (arrow to the left) is associated to the formation of mixed F127/SAIL micelles, while the second signals the formation of practically neat F127 micelles (due to the excess of polymer in the system). The low c_s observed for the first inflection point evidences strong synergism in the mixed aggregation between polymer and SAILs, since the value is much smaller than the *cmc* of both individual components. Therefore, the presence of SAIL clearly promotes mixed micelle formation. These results are thus consistent with those obtained by DSC, namely with the lower *cmt* and broadening of peaks seen in the F127/SAIL mixtures as compared to F127 alone. When the SAIL molar fraction increases to 0.80, there is only

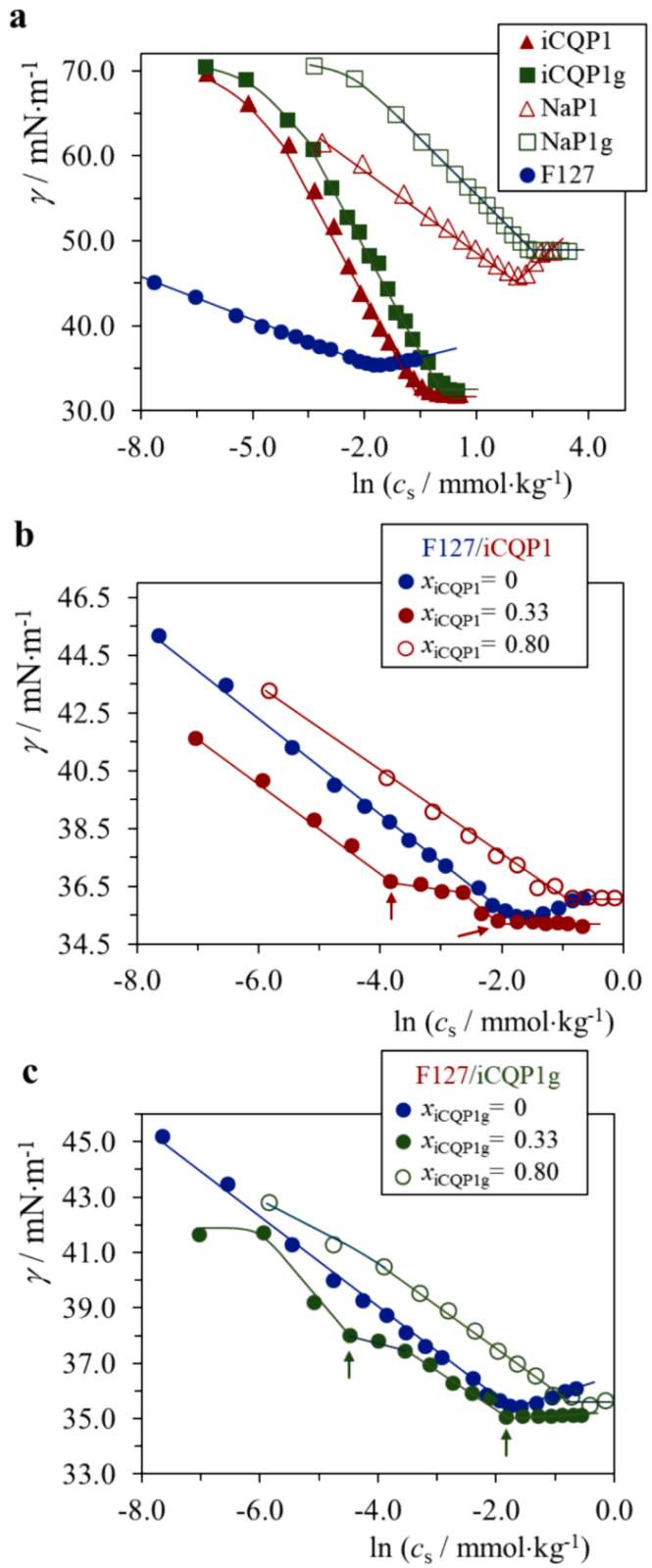

Fig. 4. Surface tension curves at 26.5 °C for: **a**, the neat compounds—polymer F127, SAILs iCQP1 and iCQP1g, sodium cholate (NaP1) and sodium glycocholate (NaP1g); **b**, F127/iCQP1 mixtures; and **c**, F127/iCQP1g mixtures. In **b** and **c** the arrows denote two critical aggregation concentrations.

Table 1
Interfacial parameters for the neat compounds and for F127/SAIL mixtures, at 26.5 °C.[1]

System	x_{SAIL}	*cmc*/mmol·kg^{-1}	$a_{s,min}$/nm^2	γ_{cmc}/mN·m^{-1}
F127	–	0.18	2.7	35.3
iCQP1	–	0.60	0.51	32.4
iCQP1g	–	0.78	0.43	33.9
NaP1	–	9.3	2.7	45.5
NaP1g	–	11.3	1.9	49.0
F127/iCQP1	0.33	0.022; 0.13	–	36.7; 35.3
	0.80	0.32	–	36.1
F127/iCQP1g	0.33	0.011; 0.16	–	38.0; 35.1
	0.80	0.51	–	35.4

[1] The *cmc* values have a typical uncertainty of ±5 %. For F127/SAIL mixtures at 0.33, the two values shown correspond to the two break points observed in the *cmc* curves (Fig. 4).

one inflection point corresponding to the mixture *cmc*. This fact denotes that only a single type of aggregate is forming, in this case mixed polymer/SAIL micelles highly enriched in SAIL. Significantly, the *cmc* lies between that of neat F127 and that of the corresponding neat SAIL, indicating that when the polymer is the major component in the mixture, the tendency for mixed micellization is weaker than when the SAIL is the major one.

3.2.3. DLS and zeta potential studies

The evolution of size of the mixed F127/SAIL micelles with x_{SAIL} was investigated by DLS and the results are shown in Fig. 5. Similar to the DSC studies, the polymer concentration in all compositions was kept fixed at 5.0 mmol·kg^{-1}, while x_{SAIL} was varied. The plots of the intensity-weighted scattering *vs.* hydrodynamic diameter (D_h) show relatively monodisperse peaks at low sizes consistent with micelles. F127 individually shows micelles with an average diameter, $\langle D_h \rangle$, of 20 nm, consistent with previous reports [51,52]. When the molar fraction of either SAIL increases between 0.33 and 0.90, the micelle size decreases gradually from 18 to 10 nm (Fig. 5), with the micelles remaining fairly monodisperse. It should be noted that attempts were made to measure neat iCQP1 and neat iCQP1g micelles also by DLS, but the results were not physically meaningful, likely due to the small size of the aggregates ($D_h < 5$ nm). The trend observed in Fig. 5 can be explained by the gradual enrichment of the mixed micelles in the small SAIL molecules. In fact, there is a considerable difference in size between F127 and the SAIL molecules herein studied. This will presumably force the polymer to pack into smaller aggregates as well, reducing the number of

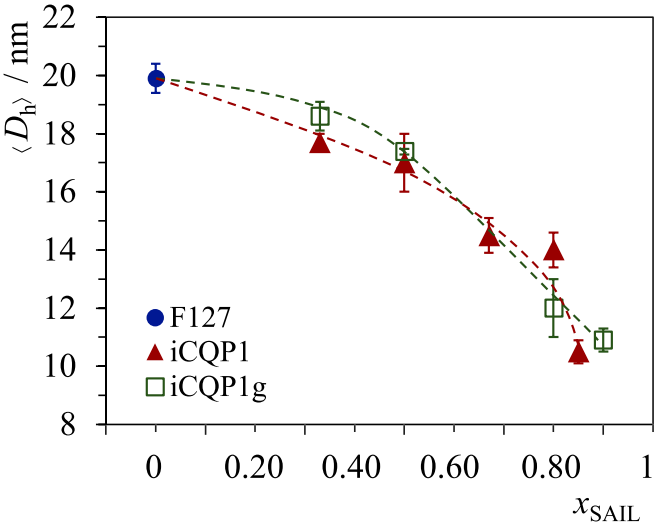

Fig. 5. Mean hydrodynamic diameter *vs.* molar fraction of SAIL for F127/SAIL mixtures, at 25.0 °C, for constant $c_{F127} = 5$ mmol·kg^{-1}.

polymer molecules per mixed micelle and thus, concomitantly, increasing the concentration of micelles. A similar reduction in micelle size has been reported when the small amphiphile sodium dodecylsulfate (SDS) was added to F127 micelles [53,54]. In one of the studies, the authors concluded that the F127 content of each aggregate decreased alongside the size of the mixed micelles, which increased in number [54]. A similar effect seems to take place in the systems herein investigated. Finally, zeta potential measurements performed for F127 and the F127/SAIL mixtures yield absolute ζ values in the order of 0 – 1 mV (cf. Table S3, S.I.), confirming the electroneutral nature both of the neat polymer and of the mixed micelles.

Taken together, results from DSC, surface tension and DLS studies clearly indicate that F127 and the chloroquine bile salt SAILs strongly interact in solution to form mixed micelles, and that this interaction is synergistic at low molar fractions of the SAILs. At the physiologically-relevant temperature of 37 °C, F127 has a very low *cmc* (μM range), which can be conveniently exploited to encapsulate SAILs in the polymeric micelles and test their antiplasmodial effect in concentrations that are also physiologically relevant (nM to μM). Therefore, the activity of SAILs-loaded F127 micelles against blood-stage *P. falciparum* parasites was evaluated *in vitro*, as described in the next section.

3.3. *In vitro* activity of SAIL-loaded F127 micelles against *P. falciparum*

To evaluate the *in vitro* activity of the SAIL-loaded in F127 micelles compared to free SAILs against a CQ-sensitive (3D7-GFP) strain of *P. falciparum* (Table 2), special conditions regarding temperature and range of concentrations of solutes were carefully chosen.

Firstly, the IC_{50} values, previously reported by us, for free iCQP1 and iCQP1g against erythrocytic forms of the *P. falciparum*, respectively, 13 and 15 nM, were considered for the establishment of a suitable SAIL concentration range to be tested, i.e., 729 – nM [10]. The polymer concentration was kept constant in each dilution series.

Secondly, the *cmc* of neat F127 was evaluated at 37.0 °C, yielding a value of 2.9 μM (cf. Fig. S1 in the S.I.). Thus, to ensure that, during the biological assays (conducted at 37 °C), F127 remains fully aggregated into micelles where SAILs can be loaded (i.e. ensuring that the fraction of free polymer molecules is very small), three F127 concentrations well above the *cmc* of neat F127 were chosen — 10, 20 and 30 μM. Moreover, the molar fraction of SAIL was, in all cases, lower than 0.07. Therefore, based on evidence (Section 3.2.2) that in presence of a small molar fraction of SAIL (0.33), the *cmc* of F127/SAILs mixtures decreases compared to the *cmc* of both F127 and SAIL, it is reasonable to assume that the *cmc* of any of the mixtures prepared for *in vitro* studies is below 2.9 μM. Hence, for any combination of F127/SAIL concentrations tested (in Table 2), conditions are met to have the SAIL molecules encapsulated in the polymeric micelles.

Thirdly, three polymer concentrations were tested individually for their ability to inhibit *P. falciparum*, yielding values of 2, 41 and 93 % inhibition, respectively, compared to control. The IC_{50} value of F127 was next found to be 14.1 μM (Table 2), which is an interesting observation, as to the best of our knowledge this intrinsic (though modest) antiplasmodial activity of F127 has never been reported. Hence, the polymer concentrations used in the biological assays also span a range of low to high antiplasmodial activity of the polymer *per se*, and this is also relevant for control and comparison purposes.

Table 2
In vitro antiplasmodial activity (IC_{50}) obtained for the F127/SAIL mixtures and neat compounds against *P. falciparum* (3D7-GFP).

System	c_{F127}/μM	IC_{50}/nM
iCQP1	–	13.4 ± 0.3
F127/iCQP1	10.0	3.7 ± 1.3
	20.0	1.9 ± 0.2
	30.0	3.2 ± 0.5
iCQP1g	–	11.7 ± 2.1
F127/iCQP1g	10.0	5.9 ± 2.1
	20.0	7.2 ± 1.7
	30.0	9.7 ± 3.3
F127	variable	(14.1 ± 0.5) × 10^3

The results for the antiplasmodial activity of the F127/SAIL mixtures are shown in Table 2 and show a clear improvement in the efficacy of the micelle-loaded SAILs compared to the free compounds, as the IC_{50} of any micelle-loaded SAIL system is consistently lower than that of the respective free SAIL. This is particularly expressive for iCQP1, which show IC_{50} values in the range 1.7 – 5 nM when encapsulated in F127 micelles, compared to the 13.4 nM value determined for the free SAIL. Encapsulation of iCQP1g in F127 micelles also improve antiplasmodial activity, though with IC_{50} values (3.8 – 13 nM) not as low as those observed for encapsulated iCQP1, but still lower than that of the free iCQP1g. Thus, overall, the antiplasmodial properties of chloroquinium bile salts are enhanced when they are encapsulated in the polymeric micelles. This is a relevant finding not only by itself, but also by the wide range of advantages recently attributed to F127-based nanomedicines [45,55,56], including the reported ability of F127 micelles to reduce drug-induced hemolysis [57].

Relevantly, the polymer concentration does not seem to play any role in the *in vitro* antiplasmodial activity, as IC_{50} values of both F127/SAIL systems remain virtually unchanged within experimental error, regardless of the concentration of F127 employed (Table 2). Since higher polymer concentration means in principle higher number of F127 micelles available for loading SAILs, we can conclude that at least for the concentration range tested, the antiplasmodial effect is independent of SAIL payload per micelle.

Finally, one question emerges: are the F127 polymeric micelles effectively acting as nanocarriers of the SAILs or could they be just facilitating the interaction of any free SAIL molecules with *Plasmodium*-infected red blood cells? Two arguments support the first case. (i) The F127 concentrations used in the assays ensure the abundance of polymeric micelles in the system and since the SAILs are amphiphiles themselves (with global hydrophobic character, as shown by their low *cmc* values), it is reasonable to assume they always prefer to be solubilized in the polymeric micelles than in the aqueous bulk. In fact, as stated before, the SAILs facilitate the micellization of F127 in a synergistic manner. (ii) Let us assume, for the sake of argument, that in some of the conditions tested (namely at very low concentrations of SAIL, near the 1 nM range, there is one of two scenarios: a) existence of neat F127 micelles, SAIL-loaded micelles, and in addition free SAIL and free F127 in the bulk; b) similar to the previous but without free SAIL molecules. Even in these scenarios, it is highly unlikely that the antiplasmodial effect is facilitated by the neat F127 micelles or by F127 unimers through some mechanism that would "open the door" to the SAILs. This is because the IC_{50} of F127 alone is 14.1 μM, which is ca. 3 orders of magnitude higher than the IC_{50} values obtained for all F127/SAIL mixtures. Hence, it is reasonable to expect that if the action of neat F127 micelles was the critical factor in promoting the SAIL activity (compared to free SAIL), the IC_{50} of F127/SAIL mixtures would necessarily be closer to that of the neat F127. This is not observed, as they are significantly lower than the IC_{50} values for the free SAILs. So, based on arguments (i) and (ii), the logical conclusion is that the enhanced antiplasmodial activity observed for SAILs when in the presence of F127 is due to the role of F127 polymeric micelles as nanocarriers for the SAIL molecules. Thus, any mechanism of action must entail the existence of these mixed aggregates.

4. Conclusion

In this work, the capacity of polymeric micelles of poloxamer F127 to act as nanocarriers for two antimalarial SAILs, iCQP1 and iCQP1g, has

been investigated. Our original hypothesis was that the antiplasmodial activity could be enhanced by encapsulating the SAILs in polymeric micelles.

The micellization properties of neat F127 and of F127/SAIL mixtures were first characterized by DSC, DLS, and surface tension measurements. The micellization of F127 is a strongly concentration and temperature-dependent process characterized by a molar enthalpy and molar entropy equal to 301 ± 8 kJ·mol^{-1} and 1015 ± 24 J·K^{-1}·mol^{-1}, respectively, both independent of polymer concentration. As the temperature is increased, the *cmc* of F127 is drastically reduced. When the molar fraction of SAIL (x_{SAIL}) in the F127/SAIL mixture is increased (between 0.33 and 0.90), at constant polymer concentration, the micellar properties of F127 are significantly changed. The overall effect is that either SAIL favors mixed micellization by decreasing both the *cmt* (as observed by DSC) and the *cmc* of the mixture (as observed by surface tension, when SAIL is the minor component, $x_{SAIL} = 0.33$). Concomitantly, the micellar size is reduced from 20 to 10 nm as x_{SAIL} is increased, as observed by DLS, implying the presence of more micelles and a larger surface area of the system. These features could be conveniently exploited to load F127 micelles with SAILs, at very low concentrations of polymer and SAIL (μM and nM, respectively) and at physiological temperature (37 °C), aiming at an enhanced efficacy of the SAILs against intraerythrocytic forms of *Plasmodium* parasites. As such, three polymer concentrations, 10, 20 and 30 μM, were tested, and the SAIL concentration was varied for each of them. Remarkably, the biological assays show that when the SAILs are loaded into the F127 polymeric micelles, the antiplasmodial efficacy is substantially enhanced, compared to both to the free SAIL (the most important aspect) and neat F127. This is clearly demonstrated by the 2.5–6.5-fold decrease in the IC_{50} value for encapsulated *versus* free iCQP1.

In conclusion, using polymeric micelles of F127 as nanocarriers enhances the biological activity of two antimalarial SAILs, paving the way to new promising formulations to combat the disease that allow the reuse of classical antimalarials like chloroquine.

CRediT authorship contribution statement

Ana Teresa Silva: Writing – original draft, Validation, Investigation, Formal analysis. **Isabel S. Oliveira:** Validation, Investigation, Formal analysis, Conceptualization. **Inês Morais:** Investigation, Formal analysis. **Sofia Santana:** Investigation, Formal analysis. **Eyob A. Workneh:** Investigation, Formal analysis. **Miguel Prudêncio:** Validation, Formal analysis. **Fátima Nogueira:** Validation, Formal analysis. **Ricardo Ferraz:** Writing – review & editing, Supervision, Resources, Funding acquisition. **Paula Gomes:** Writing – review & editing, Supervision, Resources, Funding acquisition, Conceptualization. **Eduardo F. Marques:** Writing – review & editing, Validation, Supervision, Resources, Formal analysis, Conceptualization.

Declaration of competing interest

The authors declare that they have no known competing financial interests or personal relationships that could have appeared to influence the work reported in this paper.

Acknowledgements

The authors thank Fundação para a Ciência e Tecnologia/Ministério da Educação e Ciência – FCT/MEC, for PT national funds through the project CIRCNA/BRB/0281/2019. FCT/MCE is further acknowledged for supporting the Research Units LAQV-REQUIMTE (LA/P/0008/2020, UIDP/50006/2020 and UIDB/50006/2020), CIQUP (UIDB/00081/2020), IMS (LA/P/0056/2020), and GHTM (UID/Multi/04413/2020) and LA-REAL (LA/P/0117/2020). MP further acknowledges the "la Caixa" Foundation for Grant HR21-848. ATS and IM thank both FCT/MCTES and Sociedade Portuguesa de Química (SPQ, Portugal) for their doctoral grants SFRH/BD/150649/2020 and 2023.03356.BD, respectively. The following reagent was obtained through BEI Resources, NIAID, NIH: *Plasmodium falciparum*, Strain 3D7HT-GFP, MRA-1029, contributed by Andrew M. Talman and Robert E. Sinden.

Appendix A. Supplementary material

Supplementary data to this article can be found online at https://doi.org/10.1016/j.molliq.2024.125986.

References

[1] W.H. Organization, World malaria report 2023, 2023.
[2] P.J. Rosenthal, V. Asua, M.D. Conrad, Emergence, transmission dynamics and mechanisms of artemisinin partial resistance in malaria parasites in Africa, Nat. Rev. Microbiol. 22 (2024) 373–384.
[3] J.L. Siqueira-Neto, K.J. Wicht, K. Chibale, J.N. Burrows, D.A. Fidock, E. A. Winzeler, Antimalarial drug discovery: progress and approaches, Nat. Rev. Drug Discov. 22 (10) (2023) 807–826.
[4] L.N. Borgheti-Cardoso, M. San Anselmo, E. Lantero, A. Lancelot, J.L. Serrano, S. Hernández-Ainsa, X. Fernàndez-Busquets, T. Sierra, Promising nanomaterials in the fight against malaria, J. Mater. Chem. B 8 (41) (2020) 9428–9448.
[5] N. Rao, T. Poojari, C. Poojary, R. Sande, S. Sawant, Drug repurposing: a shortcut to new biological entities, Pharm. Chem. J. 56 (9) (2022) 1203–1214.
[6] M. Rudrapal, S.J. Khairnar, G.J. Anil, Anil, Drug repurposing (DR): an emerging approach in drug discovery, in: A.B. Farid (Ed.), Drug Repurposing, IntechOpen, Rijeka, 2020.
[7] D. Fontinha, I. Moules, M. Prudêncio, Repurposing drugs to fight hepatic malaria parasites, Molecules 25 (15) (2020).
[8] A.T. Silva, I.S. Oliveira, J. Gomes, L. Aguiar, D. Fontinha, D. Duarte, F. Nogueira, M. Prudêncio, E.F. Marques, C. Teixeira, Drug-derived surface-active ionic liquids: a cost-effective way to expressively increase the blood-stage antimalarial activity of primaquine, ChemMedChem 17 (5) (2022).
[9] A.T. Silva, L. Lobo, I.S. Oliveira, J. Gomes, C. Teixeira, F. Nogueira, E.F. Marques, R. Ferraz, P. Gomes, Building on surface-active ionic liquids for the rescuing of the antimalarial drug chloroquine, Int. J. Mol. Sci. 21 (15) (2020).
[10] A.T. Silva, I. Oliveira, D. Duarte, D. Moita, M. Prudêncio, F. Nogueira, R. Ferraz, E. F. Marques, P. Gomes, "Seasoning" antimalarial drugs' action: chloroquine bile salts as novel triple-stage antiplasmodial hits, RSC Med. Chem. (2024).
[11] R.M. Moshikur, R.L. Carrier, M. Moniruzzaman, M. Goto, Recent advances in biocompatible ionic liquids in drug formulation and delivery, Pharmaceutics 15 (4) (2023) 28.
[12] E. Beaven, R. Kumar, J.M. An, H. Mendoza, S.C. Sutradhar, W. Choi, M. Narayan, Y.K. Lee, M. Nurunnabi, Potentials of ionic liquids to overcome physical and biological barriers, Adv. Drug Deliv. Rev. 204 (2024) 18.
[13] W.X. Zhang, Y.R. Gao, R. Xue, W. Nguyen, W. Chen, J.H. Wang, Y. Shu, Liquid formulations based on ionic liquids in biomedicine, Mater. Today Phys. 30 (2023) 19.
[14] J. Zhou, J. Zhang, Y.W. Sun, F.S. Luo, M. Guan, H.L. Ma, X.M. Dong, J.F. Feng, A nano-delivery system based on preventing degradation and promoting absorption to improve the oral bioavailability of insulin, Int. J. Biol. Macromol. 244 (2023) 15.
[15] A. Júlio, S.A.C. Lima, S. Reis, T.S. de Almeida, P. Fonte, Development of ionic liquid-polymer nanoparticle hybrid systems for delivery of poorly soluble drugs, J. Drug Del. Sci. Technol. 56 (2020) 6.
[16] R. Tiwari, R.P. Gupta, V.K. Singh, A. Kumar, P. Rajneesh, S. Madhukar, V. Sundar, R Kumar Gautam, Nanotechnology-based strategies in parasitic disease management: from prevention to diagnosis and treatment, ACS Omega 8 (45) (2023) 42014–42027.
[17] K. Shakeel, S. Raisuddin, S. Ali, S.S. Imam, M.A. Rahman, G.K. Jain, F.J. Ahmad, Development and in vitro/in vivo evaluation of artemether and lumefantrine co-loaded nanoliposomes for parenteral delivery, J. Liposome Res. 29 (1) (2019) 35–43.
[18] M. Marwah, P.N. Srivastava, S. Mishra, M. Nagarsenker, Functionally engineered 'hepato-liposomes': combating liver-stage malaria in a single prophylactic dose, Int. J. Pharm. 587 (2020) 119710.
[19] A. Ramazani, M. Keramati, H. Malvandi, H. Danafar, H. Kheiri Manjili, Preparation and in vivo evaluation of anti-plasmodial properties of artemisinin-loaded PCL–PEG–PCL nanoparticles, Pharm. Dev. Technol. 23 (9) (2018) 911–920.
[20] E.M. Coma-Cros, A. Lancelot, M. San Anselmo, L.N. Borgheti-Cardoso, J.J. Valle-Delgado, J.L. Serrano, X. Fernàndez-Busquets, T. Sierra, Micelle carriers based on dendritic macromolecules containing bis-MPA and glycine for antimalarial drug delivery, Biomater. Sci. 7 (4) (2019) 1661–1674.
[21] D. Bhadra, S. Bhadra, N. Jain, PEGylated peptide dendrimeric carriers for the delivery of antimalarial drug chloroquine phosphate, Pharm. Res. 23 (2006) 623–633.
[22] A. Kumari, N. Bajwa, Malaria therapeutic paradigm: an evolution towards commercial drug delivery technology, Curr. Treat. Opt. Infect. Dis. (2024).
[23] Y. Avalos-Padilla, X. Fernàndez-Busquets, Nanotherapeutics against malaria: a decade of advancements in experimental models, Wiley Interdiscip. Rev.: Nanomed. Nanobiotechnol. 16 (2) (2024).

[24] M.F. Francis, M. Cristea, F.M. Winnik, Polymeric micelles for oral drug delivery: why and how, Pure Appl. Chem. 76 (7–8) (2004) 1321–1335.
[25] S. Kotta, H.M. Aldawsari, S.M. Badr-Eldin, A.B. Nair, K. Yt, Progress in polymeric micelles for drug delivery applications, Pharmaceutics 14 (8) (2022) 1636.
[26] A.R. Fares, A.N. ElMeshad, M.A. Kassem, Enhancement of dissolution and oral bioavailability of lacidipine via pluronic P123/F127 mixed polymeric micelles: formulation, optimization using central composite design and in vivo bioavailability study, Drug Deliv. 25 (1) (2018) 132–142.
[27] W. Xu, P. Ling, T. Zhang, Polymeric micelles, a promising drug delivery system to enhance bioavailability of poorly water-soluble drugs, J. Drug Del. 2013 (2013).
[28] K. Nakashima, P. Bahadur, Aggregation of water-soluble block copolymers in aqueous solutions: recent trends, Adv. Colloid Interface Sci. 123 (2006) 75–96.
[29] C.S. da Costa, E.M. Marques, J.R. do Nascimento, V.A.S. Lima, R. Santos-Oliveira, A.S. Figueredo, C.M. de Jesus, G.C. de Souza Nunes, C.M. Brandão, E.T. de Jesus, Design of liquid formulation based on F127-loaded natural dimeric flavonoids as a new perspective treatment for Leishmaniasis, Pharmaceutics 16 (2) (2024) 5–55.
[30] S.H. Kwon, S.Y. Kim, K.W. Ha, M.J. Kang, J.S. Huh, I. Tae Jong, Y.M. Kim, Y. M. Park, K.H. Kang, S. Lee, Pharmaceutical evaluation of genistein-loaded pluronic micelles for oral delivery, Arch. Pharm. Res. 30 (2007) 1138–1143.
[31] H. Shen, S. Liu, P. Ding, L. Wang, J. Ju, G. Liang, Enhancement of oral bioavailability of magnolol by encapsulation in mixed micelles containing pluronic F127 and L61, J. Pharm. Pharmacol. 70 (4) (2018) 498–506.
[32] X. Wu, W. Ge, T. Shao, W. Wu, J. Hou, L. Cui, J. Wang, Z. Zhang, Enhancing the oral bioavailability of biochanin A by encapsulation in mixed micelles containing Pluronic F127 and Plasdone S630, Int. J. Nanomed. (2017) 1475–1483.
[33] Z. Zhang, C. Cui, F. Wei, H. Lv, Improved solubility and oral bioavailability of apigenin via Soluplus/Pluronic F127 binary mixed micelles system, Drug Dev. Ind. Pharm. 43 (8) (2017) 1276–1282.
[34] P. Valissery, R. Thapa, J. Singh, D. Gaur, J. Bhattacharya, A.P. Singh, S.K. Dhar, Potent *in vivo* antimalarial activity of water-soluble artemisinin nano-preparations, RSC Adv. 10 (59) (2020) 36201–36211.
[35] P.A. Hassan, S. Rana, G. Verma, Making sense of Brownian motion: colloid characterization by dynamic light scattering, Langmuir 31 (1) (2015) 3–12.
[36] S. Bhattacharjee, DLS and zeta potential–what they are and what they are not? J. Control. Release 235 (2016) 337–351.
[37] F. Nogueira, A. Diez, A. Radfar, S. Pérez-Benavente, V.E. do Rosario, A. Puyet, J. M. Bautista, Early transcriptional response to chloroquine of the Plasmodium falciparum antioxidant defence in sensitive and resistant clones, Acta Trop. 114 (2) (2010) 109–115.
[38] M. Machado, F. Murtinheira, E. Lobo, F. Nogueira, Whole-Cell SYBR Green I assay for antimalarial activity assessment, Ann. Clin. Med. Microbiol. 2 (1) (2016).
[39] S.A. Milheiro, J. Gonçalves, R.M. Lopes, M. Madureira, L. Lobo, A. Lopes, F. Nogueira, D. Fontinha, M. Prudêncio, M.F.M. Piedade, Half-sandwich cyclopentadienylruthenium (II) complexes: a new antimalarial chemotype, Inorg. Chem. 59 (17) (2020) 12722–12732.
[40] A. Torcello-Gomez, J. Maldonado-Valderrama, A.B. Jódar-Reyes, T.J. Foster, Interactions between pluronics (F127 and F68) and bile salts (NaTDC) in the aqueous phase and the interface of oil-in-water emulsions, Langmuir 29 (8) (2013) 2520–2529.
[41] A.A. Barba, M. d'Amore, M. Grassi, S. Chirico, G. Lamberti, G. Titomanlio, Investigation of Pluronic© F127-water solutions phase transitions by DSC and dielectric spectroscopy, J. Appl. Polym. Sci. 114 (2) (2009) 688–695.
[42] J. Jansson, K. Schillén, G. Olofsson, R.C. da Silva, W. Loh, The interaction between PEO-PPO-PEO triblock copolymers and ionic surfactants in aqueous solution studied using light scattering and calorimetry, J. Phys. Chem. B 108 (1) (2004) 82–92.
[43] E. Feitosa, F.M. Winnik, Interaction between Pluronic F127 and dioctadecyldimethylammonium bromide (DODAB) vesicles studied by differential scanning calorimetry, Langmuir 26 (23) (2010) 17852–17857.
[44] L.C. Salay, E.A. Prazeres, N.S.M. Huachaca, M. Lemos, J.P. Piccoli, P.R.S. Sanches, E.M. Cilli, R.S. Santos, E. Feitosa, Molecular interactions between Pluronic F127 and the peptide tritrpticin in aqueous solution, Colloid Polym. Sci. 296 (4) (2018) 809–817.
[45] R.A. Gutiérrez-Saucedo, J.C. Gómez-López, A.A. Villanueva-Briseño, A. Topete, J.F. A. Soltero-Martínez, E. Mendizábal, C.F. Jasso-Gastinel, P. Taboada, E.B. Figueroa-Ochoa, Pluronic F127 and P104 polymeric micelles as efficient nanocarriers for loading and release of single and dual antineoplastic drugs, Polymers 15 (10) (2023) 19.
[46] P. del Burgo, E. Aicart, E. Junquera, Mixed vesicles and mixed micelles of the cationic-cationic surfactant system: didecyldimethylammonium bromide/ dodecylethyldimethylammonium bromide/water, Colloid Surf. A-Physicochem. Eng. Asp. 292 (2–3) (2007) 165–172.
[47] I. Grillo, J. Penfold, I. Tucker, F. Cousin, Spontaneous formation of nanovesicles in mixtures of nonionic and dialkyl chain cationic surfactants studied by surface tension and SANS, Langmuir 25 (7) (2009) 3932–3943.
[48] B.V. Shankar, A. Patnaik, PH-dependent chiral vesicles from enantiomeric sodium 2,3-bis(decyloxy) succinate in aqueous solution, Langmuir 23 (7) (2007) 3523–3529.
[49] S.G. Silva, M.L.C. do Vale, E.F. Marques, Size, charge, and stability of fully serine-based catanionic vesicles: towards versatile biocompatible nanocarriers, Chem.-Eur. J. 21 (10) (2015) 4092–4101.
[50] M. Villeneuve, S. Kaneshina, T. Imae, M. Aratono, Vesicle-micelle equilibrium of anionic and cationic surfactant mixture studied by surface tension, Langmuir 15 (6) (1999) 2029–2036.
[51] C. Popovici, M. Popa, V. Sunel, L.I. Atanase, D.L. Ichim, Drug delivery systems based on Pluronic micelles with antimicrobial activity, Polymers 14 (15) (2022) 15.
[52] D. Patel, S.L. Gawali, K. Kuperkar, P.A. Hassan, P. Bahadur, Co-micellization conduct and structural dynamics of block copolymers in water and salt solution environment for drug solubilization enhancement, Colloid Polym. Sci. 301 (8) (2023) 919–931.
[53] E. Hecht, K. Mortensen, M. Gradzielski, H. Hoffmann, Interaction of ABA block copolymers with ionic surfactants: influence on micellization and gelation, J. Phys. Chem. 99 (13) (1995) 4866–4874.
[54] Y. Li, R. Xu, D. Bloor, J. Holzwarth, E. Wyn-Jones, The binding of sodium dodecyl sulfate to the ABA block copolymer Pluronic F127 (EO97PO69EO97): an electromotive force, microcalorimetry, and light scattering investigation, Langmuir 16 (26) (2000) 10515–10520.
[55] B. Klahan, N. O'Reilly, A. Chauhan, H.H. Sigurdsson, S. Mering, L. Fitzhenry, Micellar solutions of Pluronic F127 for ocular drug delivery, Acta Ophthalmol. 100 (2022) 1.
[56] N.U. Khaliq, J. Lee, S. Kim, D. Sung, H. Kim, Pluronic F-68 and F-127 based nanomedicines for advancing combination cancer therapy, Pharmaceutics 15 (8) (2023) 25.
[57] V.A. Feitosa, V.C. de Almeida, B. Malheiros, R.D. de Castro, L.R.S. Barbosa, N.N. P. Cerize, C.D. Rangel-Yagui, Polymeric micelles of pluronic F127 reduce hemolytic potential of amphiphilic drugs, Colloid Surf. B-Biointerfaces 180 (2019) 177–185.